SCIENCE LETTERS

eISSN: 2682-8626

Available online at
https://scilett-fsg.uitm.edu.my/

Science Letters 18(2) 2024, 28 – 43.

Science Letters

Effect of Montmorillonite Nanofiller Loading on The Properties of The Hemicellulose Blend Carboxymethyl Cellulose Nanocomposite Films

Hanis Madihah Abd Munir[1], Mohd Zaim Jaafar[1], Nasrullah Razali[3], Mohamad Haafiz Mohamad Kassim[1,2]*, Falah Abu[4,5]*, Nurul Fazita Mohammad Rawi[1], Nur Adilah Abu Hassan[2]

[1] *Bioresource Technology Division, School of Industrial Technology, Universiti Sains Malaysia, 11800 Penang, Malaysia.*
[2] *Cluster of Green Biopolymer, Coatings & Packaging, School of Industrial Technology, Universiti Sains Malaysia. 11800 Minden, Pulau Pinang, Malaysia.*
[3] *Department of Chemical Engineering, Syiah Kuala University Banda Aceh, 23111 Indonesia.*
[4] *Department of Ecotechnology, School of Industrial Technology, Faculty of Applied Sciences, Universiti Teknologi MARA.*
[5] *Smart Manufacturing Research Institute (SMRI), Universiti Teknologi MARA (UiTM) Shah Alam, 40450 Shah Alam, Selangor, Malaysia.*

ARTICLE INFO

Article history:
Received 12 January 2024
Revised 25 March 2024
Accepted 1 April 2024
Online first
Published 24 June 2024

Keywords:
Oil palm empty fruit bunch
Hemicelluloses
Montmorillonite
Carboxymethyl cellulose
Solution casting

DOI:
10.24191/sl.v18i2.25392

ABSTRACT

A nanocomposite film was successfully prepared by the combination of hemicellulose (H) derived from the oil palm empty fruit bunch (OPEFB) and carboxymethyl cellulose (CMC) with montmorillonite (MMT) at different loadings (1, 3, and 5 wt%) through solution casting. The composites were characterized by using scanning electron microscope (SEM), x-ray diffraction (XRD), contact angle, and Fourier transform infrared (FTIR) analysis. The results showed that the tensile properties of the H-CMC-MMT nanocomposite films were enhanced at 3 wt% MMT loading. Scanning electron microscopy displayed a smooth surface of the nanocomposite film at a lower filler loading and a rough surface when the MMT loading increased. Meanwhile, the film with 3 wt% MMT exhibited the highest contact angle value, representing the lowest wettability characteristic. Thermal analysis through their thermogravimetry analysis (TGA), derivative thermogravimetry (DTG), and differential scanning calorimetry (DSC) results showed that good thermal properties were achieved as the MMT loading percentage increased. Overall, the 3% MMT in the nanocomposite formulation had optimum properties related to enhanced surface functionality and tensile properties of the hemicellulose-based nanocomposite films. The results showed that the hemicellulose films have the potential to be used for green coating and packaging applications.

* Corresponding authors. *E-mail addresses*: mhaafiz@usm.my and falah@uitm.edu.my

INTRODUCTION

Plastics are a variety of synthetic or semi-synthetic materials that use polymers as the main component. Natural fibers have recently undergone intensive exploration, as the globe is in a critical situation due to significant environmental pollution. Jute, Kenaf, Flax, Banana, Hemp, Henequen, Sisal, Ramie, and Oil Palm are a few examples of natural fibers gaining popularity as alternatives to conventional fibers usage [1,2]. Due to its annual production of million tonnes of oil palm idle waste, Malaysia has an excellent opportunity to become a country with the advantage of overcoming environmental pollution, such as plastic, by producing biodegradable packaging made up from oil palm waste. Oil Palm waste, such as empty fruit bunch (EFB), is readily available and obtained due to low market demand. Cellulose, hemicellulose, and lignin are part of this lignocellulosic material, and they can be explored as new materials to replace plastic materials [3]. The chemical composition of oil palm empty fruit bunch (OPEFB) is approximately 44.2% cellulose, 33.5% hemicellulose, and 20.4% lignin [4]. Of these three significant biopolymers, the application of hemicellulose has received the slightest consideration [5,6].

Apart from cellulose, hemicelluloses represent a complex group of polysaccharides in the plant cell wall. Due to favorable properties such as biodegradability, hydrophilicity, transparency, biocompatibility, non-toxicity, and low cost, hemicellulose-based materials have been found to have potential applications mainly in consumer packaging, membrane separation processes, as well as biomedicine [6]. Nevertheless, hygroscopicity, poor mechanical strength, and barrier properties such as brittleness and weak strength have restricted their application in the material field [7]. To overcome the above concerns, extensive attempts have been made to enhance the properties of films based on hemicelluloses, such as chemical alteration, pre-treatment, and addition of plasticizers [8].

Hemicellulose-based films are famous for their outstanding gas barrier properties, as they can create a dense low-mobility macromolecular network, and their high oxygen barrier properties make them valuable for film packaging applications [9]. However, hemicellulose-based films are hygroscopic with low mechanical strength, flexibility, and a low moisture barrier [7]. Thus, chemical alteration needs to be implemented to modify the properties of the parent compounds [10]. One of the techniques is to blend hemicellulose-based films with other biopolymers, such as carboxymethyl cellulose (CMC) [6].

Carboxymethyl cellulose is a cellulose derivative formed in an organic medium produced from the reaction between alkali cellulose with monochlorine acetate or its sodium salt. With the incorporation of CMC, excellent properties of hemicellulose films will be attained since the addition of CMC can provide transparency and high mechanical strength. CMC has a hydrophobic polysaccharide backbone and shows amphiphilic properties in most hydrophilic groups [11]. Thus, the films composed of hemicellulose and CMC blend have been reported to result in high transmittance and excellent barrier characteristics [12].

However, with only CMC in the hemicellulose film mixture, the mechanical and thermodynamic properties of the film still need to be improved for packaging purposes [12]. A way to obtain a high barrier oxygen gas permeability is to incorporate a nanoscale filler with the hemicellulose film to produce a nanocomposite hemicellulose film. The addition of nanoparticle fillers into the CMC films, such as SnO_2, ZnO, graphene oxide, and montmorillonite (MMT), is proven to enhance the thermal stability, mechanical properties, surface roughness and the glass transition temperature of the obtained nanocomposite films. The enhancement of the film properties is credited to the efficient binding of CMC to the surface of the nanoparticles with the presence of heavy hydrogen bonding, which restricts the segmental mobility of the CMC [13].

https://doi.org/10.24191/sl.v18i2.25392

Among the fillers above, montmorillonite (MMT) is a tremendous reinforcement filler that can improve the film's mechanical and water barrier properties [14]. As a nanofiller for CMC alteration, MMT is the most frequently used clay due to its abundance [15]. Besides, the introduction of MMT in the hemicellulose film solution can decrease the flammability and boost the heat tolerance with a very low loading (2–5 wt%). Moreover, MMT can form a stable suspension in water because it is a member of the family of 2:1 phyllosilicate. Since MMT is known for its hydrophilic properties, it also facilitates the distribution of this crystalline inorganic layer in water-soluble polymers [10].

As the hemicellulose in OPEFB has been shown to have a high potential value-added as a natural barrier for packaging films and predictably for the production of biodegradable plastics, this biopolymer waste can be fully utilized with minimal environmental impact [6, 16]. However, there have yet to be detailed studies on the effect of montmonrillonite (MMT) loading on the nanocomposite film's tensile, thermal, and physical properties. Thus, the optimum percentage of montmorillonite (MMT) must be added to enhance the nanocomposite film for various applications with high strength, stiffness, ductility, and sound oxygen barrier. This study aimed to assess the performance of the hemicellulose from OPEFB blend CMC nanocomposite films with the addition of MMT nanofiller and to investigate the impact of different percentages of MMT on the mechanical, thermal, and physical properties of the nanocomposite film.

EXPERIMENTAL DETAILS

Materials

Oil palm empty fruit bunch (OPEFB) was obtained from United Oil Palm Sdn Bhd, Nibong Tebal, Penang, Malaysia. Carboxymethyl cellulose (CMC) was purchased from Drex-Chem (M) Sdn Bhd, Petaling Jaya Selangor, Malaysia, and organo-modified montmorillonite (MMT) (Nanomer 1.30TC) was purchased from Nanocor Inc., Arlington Heights IL., USA. Nanomer 1.30 TC is organically modified, contains 30 wt% octadecylamine, and has a mean dry particle size of 16-22 mm.

Pulping

The pulping process was achieved using a digestor (model IBSUTEK ZAT 92). OPEFB was treated with 26% NaOH at a ratio of 1:8 (OPEFB:Liquor) at 170 ℃ for 2 h. A hydro pulper was then used to refine the pulp, which was washed with water, screened, dried, and denoted as OPEFB-P.

Holocellulose production

A total of 5 g of pulp from OPEFB-P was transferred into a 1000 ml conical flask, and 160 mL of distilled water, 1.5 g of sodium chlorite ($NaClO_2$), and 10 drops of acetic acid (10% wt/v) were added. The sample was kept inside the water bath at 70 ℃ for 3 h. 1.5 g of $NaClO_2$, 10 drops of acetic acid, and 160 ml of distilled water were added alternately for each h. After 3 h, cooled distilled water was added to stop the chemical reaction in the flask. The precipitate was then filtered with a glass crucible (2G2). The remaining pulp in the glass crucible was washed using cold distilled water followed by acetone and left to dry in the oven for 24 h.

Hemicellulose extraction from oil palm empty fruit bunch

A total of 5 g of holocellulose pulp was weighed, and 50 ml of 1.0 M NaOH was added to the beaker. Then, the mixture was heated at 40 ℃ using an oval magnetic stirrer at 800 rpm for 4 h. After 4 h, the mixture was filtered by using a filter funnel. After that, ethanol was added three times to the supernatant to precipitate the hemicelluloses. The mixture was kept in the refrigerator for 24 h.

https://doi.org/10.24191/sl.v18i2.25392

Preparation of hemicellulose-based nanocomposite film

The hemicelluloses (based on wt%) were dissolved in 20 mL distilled water inside a 250 mL conical flask, and then CMC and MMT were added slowly into the hemicellulose solution. The mixture was heated at 65 ℃ for 3 h under moderate agitation. Then, the solution was poured into a petri dish to obtain the nanocomposite film. The obtained film was oven-dried at 40 ± 0.5 ℃ for 24 h. The dried films were kept in the conditioning room prior to any analysis. The formulation of the nanocomposite films is summarised in Table 1. At first, the amount of hemicelluloses and 20 ml distilled water were put into the conical flask, followed by the addition of CMC and MMT.

Table 1. Formulation for the hemicellulose nanocomposite films.

Sample	Hemicellulose (%)	Carboxymethyl cellulose (%)	Montmorillonite (%)
60H-40CMC	60	40	0
60H-40CMC-1MMT	60	40	1
60H-40CMC-3MMT	60	40	3
60H-40CMC-5MMT	60	40	5

Characterisation and Testing

Contact angle analysis

The contact angle was determined using a Drop Shape Analyser DSA 100 goniometer (Kruss GmbH, Hamburg, Germany). Water was used as the medium for this analysis. The image of the droplet was recorded for 60 s for 60H-40CMC, 60H-40CMC-MMT, 60H-40CMC-3MMT, and 60H-40CMC-5MMT.

Fourier transform infrared (FTIR) analysis

Fourier transform infrared (FTIR) spectroscopy was performed using a Nicolet Avatar Model 360 spectrometer Fourier transform infrared spectrometer (Thermo Nicolet Corporation, Madison, WI, USA). The infrared spectrums were obtained within the 4000-500 cm^{-1} wave number range.

Scanning electron microscopy (SEM)

The tensile fracture surfaces of the composite sample were examined by scanning electron microscopy (SEM, Leica Cambridge S-360, UK). The samples were placed on the SEM holder using double-sided electrically conducting carbon adhesive tape and gold-coated with a Polaron SEM coating unit (UK). The SEM micrographs were obtained under conventional secondary imaging with an acceleration voltage of 10 kV.

Tensile testing

The tensile test was conducted according to ASTM D882 using a Texture Analyzer (Stable Micro Systems TA. XT plus, Survey, UK) with 150 mm × 300 mm (width x length) sample dimensions. The tensile strength (TS) was recorded. The film strip was clamped between the tensile grips with an initial grip separation of 100 mm, and the test speed was set at 0.8 mm s^{-1} using a load cell of 30 kg. The average result of five replicates was recorded.

https://doi.org/10.24191/sl.v18i2.25392

Differential scanning calorimetry (DSC)

Differential scanning calorimetry was analyzed using a Perkin Elmer Pyris 7 thermal analyzer (Radeberg, Germany). The sample was heated at 10 ℃/min in a nitrogen flux from 30 ℃ to 400 ℃. Eventually, as the temperature rose, the sample attained its melting point (Tm). The melting process produced an endothermic peak in the DSC curve.

Thermogravimetric analysis (TGA)

A 10 mg sample was heated at 10 ℃/min in a nitrogen flux (20 mL/min) from room temperature to 600 ℃ using a Perkin Elmer-YGA 7 Thermogravimetric Analyser (Texas, US). A thermogram recorded the percentage of sample weight loss versus temperature. Over the temperature and time intervals, the sample's mass change was continuously monitored. The samples' weight loss (T_{10}, T_{60}, and T_{max}) was calculated as a function of temperature.

RESULTS AND DISCUSSION

Wettability

As one of the basic wetting properties, the contact angle of water droplets measures the degree of hydrophilicity or hydrophobicity of the film's surface, which is generally used to estimate the film's resistance against liquid water [17]. The wettability of a liquid is how much it spreads over the surface of a particular solid, measured by the flatness of a droplet on the solid surface. It can be evaluated by measuring the contact angle [18]. The high value of contact angle θ implies a greater cohesive strength within the bulk water. Therefore, weak liquid-solid interaction occurs and causes poor wetting. On the contrary, the spreading tendencies in solids for the low value of the contact angle θ show strong solid-liquid interaction. The forces associated with the interaction of water with a surface are more significant than the cohesive strength associated with bulk liquid water [17]. The wettability can be assumed to be good when the contact angle θ is below 90°.

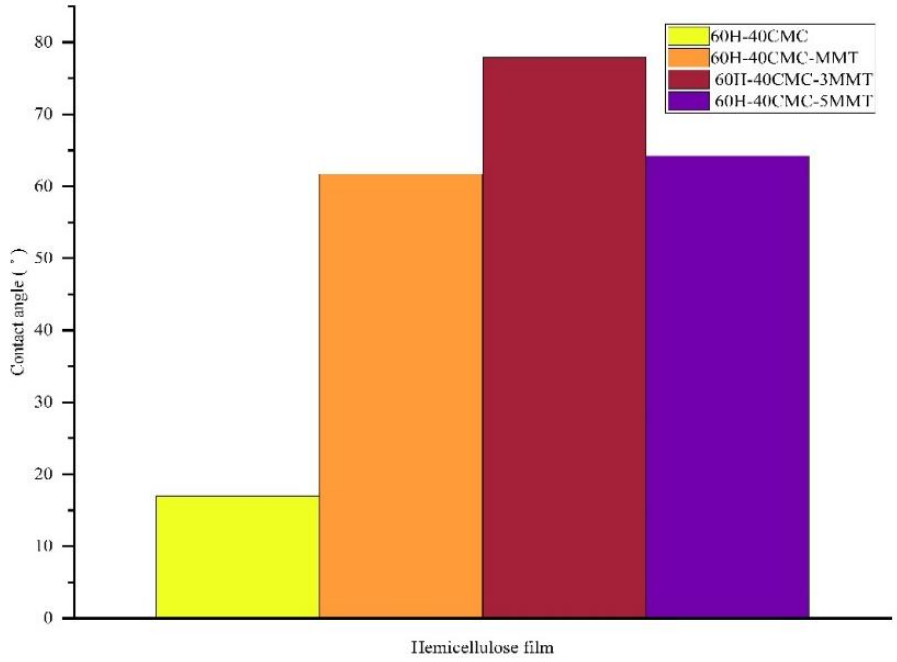

https://doi.org/10.24191/sl.v18i2.25392

Fig. 1. The contact angle of hemicellulose and nanocomposite films.

Table 2. Contact angle of hemicellulose and nanocomposite films.

Samples	Contact Angles^{o}
60H-40CMC	16.97 ± 0.8
60H-40CMC-MMT	61.69 ± 0.8
60H-40CMC-3MMT	77.93 ± 0.8
60H-40CMC-5MMT	64.23 ± 0.8

The contact angle results for the blended and nanocomposite films are shown in Figure 1 and Table 1. A significant difference can be observed for each film formulation composed of hemicellulose, CMC, and MMT. The highest degree value obtained is 77.93° by nanocomposite film, incorporating 3% MMT. The result showed the enhancement of hydrophobicity with the presence of MMT loading, which increased the contact angle of the nanocomposite film. The existence of ordered scattered nanoparticle layers with broad aspect ratios and strong dispersion of the clay platelets in the polymer matrix may cause an increase in the water contact angle of the nanocomposite film [19]. Haafiz et al. [6] facilitated this by integrating MMT into the hemicellulose-CMC blend method to improve the film's contact angle. However, incorporating CMC in the hemicellulose film with 1% MMT loading has the slightest contact angle degree with a degree value of 61.59 ^{o} compared to 3% and 5% MMT loading, resulting in the least hydrophobic specimen. Figure 1 shows that the contact angle of water droplets on a 1% MMT loading surface is smaller than the water droplet angle on the film's surface for 3% and 5% MMT loading. Thus, it can be related to the theory of contact angle measurements, which states that the narrower the contact angle, the greater the wetting propensity of a substance. The liquid will spread or wet well if the degree of contact angle is low. Meanwhile, the high degree of value will result in poor wetting [17].

Fourier transform infrared (FTIR) analysis

Figure 2 displays the FTIR spectra of the modified hemicellulose-CMC-based nanocomposite films with different loadings of MMT. The IR peaks at 3622 and 3620 cm^{-1} correspond to the -OH stretching bond of the hemicellulose-based composite. Those in the broad absorption band at about 3500 cm^{-1} are due to the stretching frequency of the hydroxyl group (-OH) [20]. The Si-O and Al-OH main functional groups representing MMT are observed in the 1000–500 cm^{-1} range. The broadband with a maximum of 1008 cm^{-1} and a small peak of 912 cm^{-1} corresponds to Si-O and Al-O stretching vibrations and is characteristic of the MMT.

A strong band at 3622 cm^{-1} and 3620 cm^{-1} shows the presence of a hydroxyl linkage. At the same time, the broadband at 3456–3448 cm^{-1} and bands at 1651–1641 cm^{-1} in the clay spectrum indicate the possibility of water hydration or H-O-H bending of water in the adsorbent. The structural -OH groups occurring in the clay mineral contribute to the shoulders and broadness of the -OH band. However, the chemical structure of this clay mineral is clearly shown by the maximum location of the band. Thus, the most crucial absorption bands that are needed for identification of the MMT clay are 3630 cm^{-1}, 3427 cm^{-1}, 1049 cm^{-1}, 918 cm^{-1}, and 524 cm^{-1} [21]. This range of absorption bands is consistent with earlier research by Madejova et al. [22].

https://doi.org/10.24191/sl.v18i2.25392

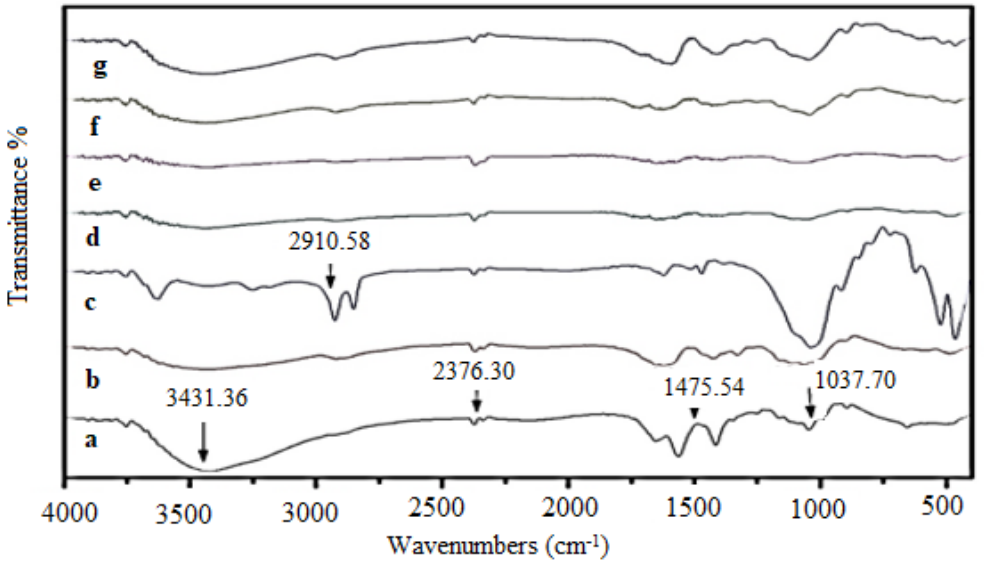

Fig. 2. FTIR spectra of H-CMC and H-CMC-MMT films; (a) Hemicellulose, (b) CMC, (c) MMT, (d) 60H-40CMC, (e) 60H-40CMC-MMT, (f) 60H-40CMC-3MMT, and (g) 60H-40CMC-5MMT.

The signals in the FTIR spectra for hemicelluloses and CMC at 3431 cm^{-1} and 2883 cm^{-1} indicate the stretching of the OH groups and the C-H vibration band. The signals present in the 1608–906 cm^{-1} range show the characteristic peaks of hemicelluloses, which is the -COO- of uronic acid and uronic carboxylates in hemicelluloses and β-glycosidic linkages between the xylose units, respectively. In the spectrum of CMC, the absorption peak at 1616 cm^{-1} is assigned to the asymmetrical -COO- stretching. The signals at 1431 cm^{-1} and 1332 cm^{-1} are related to the symmetrical stretching vibrations of the carboxylate groups and C-H bending. The broad peak at 1076 cm^{-1} is assigned to the stretching of C-O-C. When the spectra of the nanocomposite film peaks f and g are compared to that of hemicelluloses and CMC, it can be seen that the peak of the C-O-C is narrowed and shifted to the right from 1076 to 1031 cm^{-1}.

The absorption peaks at 1591 cm^{-1} and 893 cm^{-1} are seen in the FTIR spectra for the 3% and 5% MMT films. They are attributed to the asymmetrical COO-stretching and β-glycosidic bond, respectively. As the percentage of MMT increases, the peak at 3649 cm^{-1} shifts to the left, attributed to the Al-OH stretching vibration. The band at 1028 cm^{-1}, which indicates the Si-O-Si stretching vibration, has shifted to the right up to 1033 cm^{-1}. The peak at 1629 cm^{-1} to 1606 cm^{-1} indicates the presence of the –OH bending vibration. Overall, 60H-40CMC-5MMT showed the most significant spectrum and formed the most robust interfacial attachment needed for stress transfer among all the nanocomposite films, followed by 60H-40CMC-3MMT and 60H-40CMC-MMT.

X-ray diffraction (XRD) analysis

X-ray diffraction techniques (XRD), as shown in Figure 3, examined the phase purity and crystallinity of hemicellulose-based nanocomposite film. Composite films (e-f) show a typical diffractogram of a CMC-MMT composite with a broad diffraction peak at $2\theta = 11.23^{o}$, $2\theta = 19.50^{o}$, as partially crystalline behavior. Small peaks can be seen in blend film (a), (b), and composite film (d). This is because hemicellulose nanocomposite films are semi-crystalline and hygroscopic compared to

https://doi.org/10.24191/sl.v18i2.25392

hemicellulose, which is an amorphous character 24. The MMT graph (c) indicates 2:1 swelling clay at 2 θ = 26.69°, 2 θ = 34.83°. The film crystallinity increased as the MMT concentration increased from 2 θ = 20.01° to 2 θ = 26.34°. The layer structures are formed when polymer chains are built between the clay layers and fit between the two phases of crystalline and amorphous structure. Thus, it allows the peak expansion of the XRD or shifts to smaller angles. As for the XRD pattern of the amorphous behavior, the parallel between clay layers and the sheets has been removed due to discrete clay layers, which will further affect the polymer of the clay layers [23].

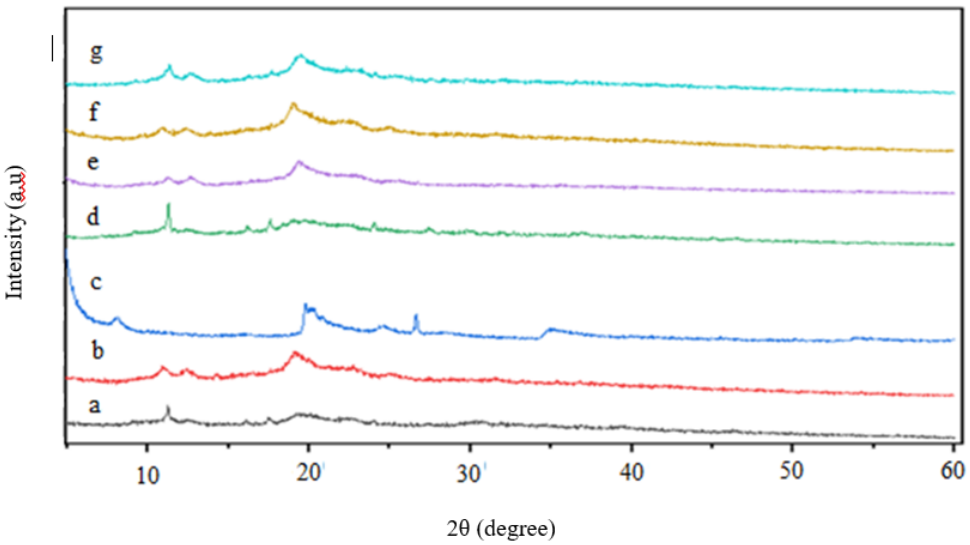

Fig. 3 displays an X-ray diffraction (XRD) graph of the blend and nanocomposite films: (a) Hemicelluloses, (b) CMC, (c) MMT, (d) 60H-40CMC, (e) 60H-40CMC-MMT, (f) 60H-40CMC-3MMT, (g) 60H-40CMC-5MMT.

Tensile properties

Figure 4 illustrates the mechanical properties of the H-CMC film blend with the MMT. The tensile strength of MMT nanoblend film first increased and decreased with the addition of MMT content. The highest tensile strength value obtained is 13.04 MPa at 3% of MMT in the blend H-CMC film. However, the effect of MMT was reduced by adding 5% of MMT into blend H-CMC film in the concentration of H-CMC. The improvement in Tensile Strength of nanocomposite in low amounts of MMT may attributed to the uniform dispersion of MMT in H-CMC blend film [24]. The interfacial interaction between the film matrix and MMT filler is enhanced with an increase in MMT loading. The decrease in Tensile Strength at high concentrations of MMT or the occurrence of partial agglomeration led to a decrease in the reinforcing effect of MMT [24].

https://doi.org/10.24191/sl.v18i2.25392

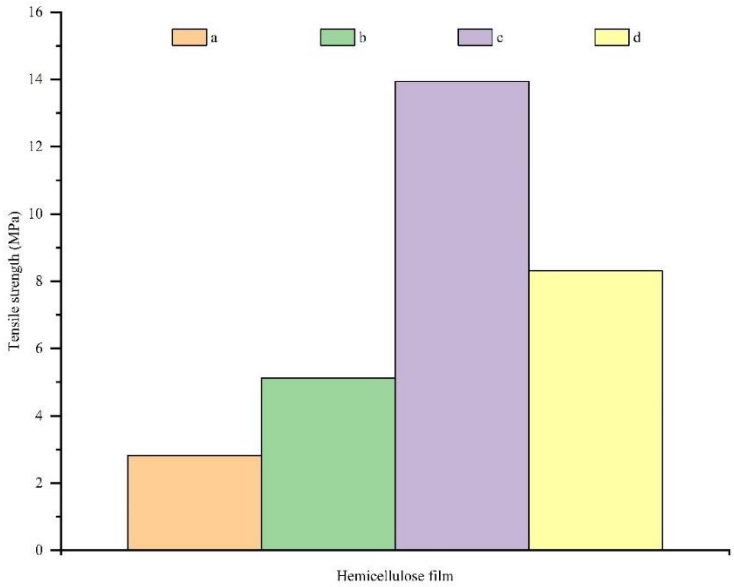

Fig.4. Tensile strength of the blend and nanocomposite films; (a) 60H-40CMC, (b) 60H-40CMC-MMT, (c) 60H-40CMC-3MMT, (d) 60H-40CMC-5MMT.

Table 3. Tensile strength of the blend and nanocomposite films.

Samples	Tensile Strength (MPa)
60H-40CMC	2.83 ± 0.63
60H-40CMC-MMT	5.12 ± 0.69
60H-40CMC-3MMT	13.94 ± 0.72
60H-40CMC-5MMT	8.31 ± 1.8

A similar result has been reported earlier by Rosnan and Arshad [24]. When MMT was incorporated into the PET/HDPE blend nanocomposite, the tensile strength of the blend reached a peak of 3% and began to decrease beyond 3% of the MMT load used. With the addition of 5% MMT, the film strength was further reduced due to organoclay agglomeration at the high loading, which can cause local stress concentration in the composite structure. Moreover, in the higher loading, the MMT dispersion could be more optimal, and incomplete intercalation decreases the properties of the nanocomposite film [24].

The SEM micrographs of the tensile cross-sectional fracture surface of hemicelluloses with CMC and the incorporation of MMT (Figure 5) explain the result. The 60H-40CMC-MMT film, as well as the 60H-40CMC-3MMT film, displayed a dense, smooth, and homogeneous formation without remarkable discontinuities or aggregates except for the pores found in Figure 5(c), which may be due to the small lump of MMT when an external force was applied. The 60H-40CMC film without MMT shows an uneven blend structure due to the porosity inside the film. However, for the maximum loading of MMT (60H-40CMC-5MMT), the film was rough, porous, and had the most uneven formation of the nanocomposite surface.

https://doi.org/10.24191/sl.v18i2.25392

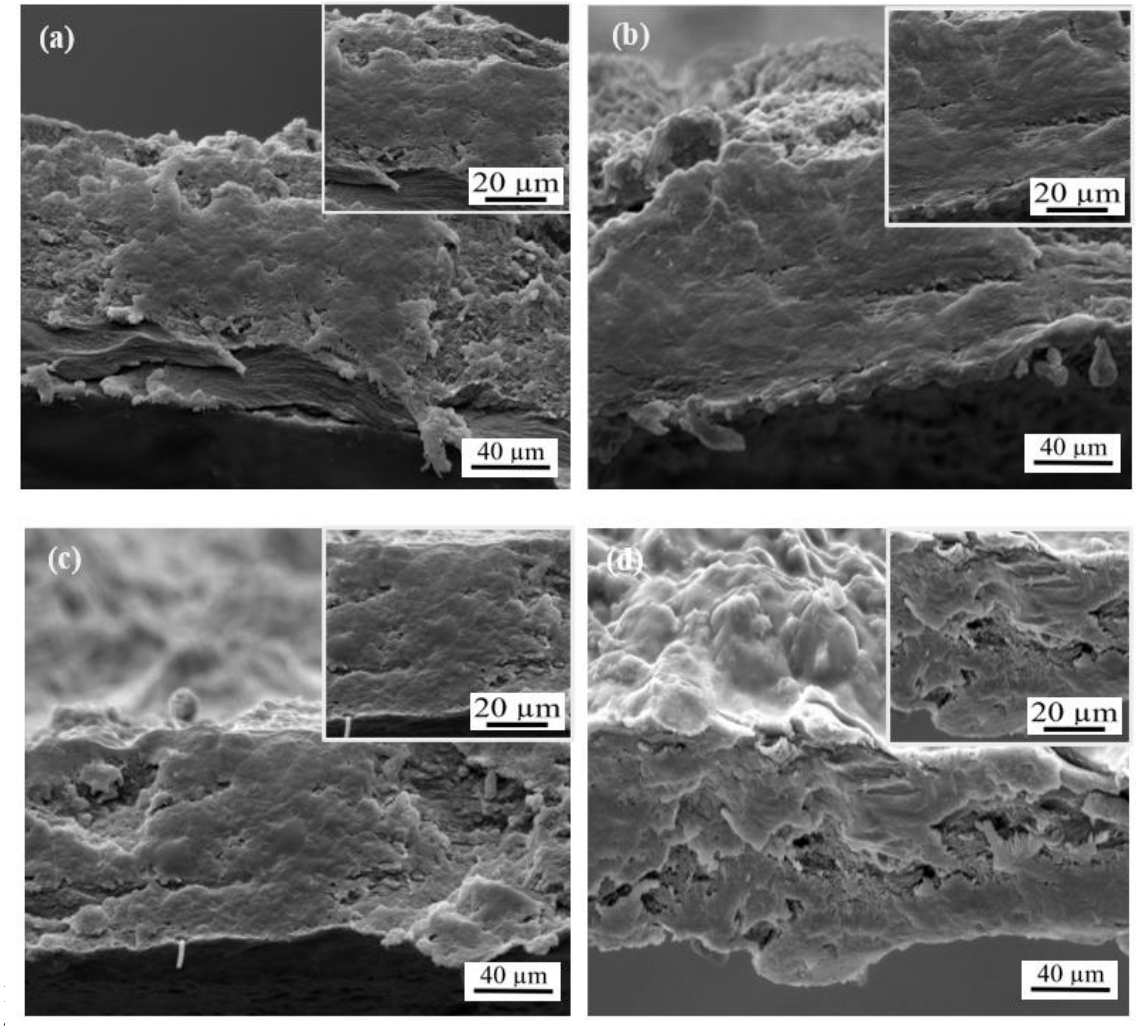

The modification of the hemicellulose film proved that with the addition of 3% MMT concentration in the film, the properties of the hemicellulose film are enhanced when the MMT filler is well dispersed in the polymer matrix. Fig. 5 shows that adding 1% and 3% of MMT loading resulted in a dense, smooth, and homogenous formation. MMT is a layered silicate with a high surface area and is negatively charged [25]. Therefore, incorporating hemicelluloses, hydrogen bonding, and electrostatic attraction between the oppositely charged polymers is the driving force for developing tight and smooth films [12]. This has been proven by the results showing that 3% MMT exhibits the highest tensile strength compared to blend films, 1% and 5% MMT.

Differential scanning calorimetry (DSC)

Hemicellulose film is well-known for its amorphous character. It is necessary to enhance its crystallization rate to use it as an engineering polymer. The effect of MMT on the crystallization behavior of hemicellulose-based film during heating and melting is examined by DSC. In DSC, glass transition temperature (T_g) and melting temperature (T_m) are two parameters that can characterize the amorphous and

https://doi.org/10.24191/sl.v18i2.25392

crystallization rate. The heat flow with increasing temperature using DSC was measured for nanocomposite films. The data were plotted as presented in Figure 6.

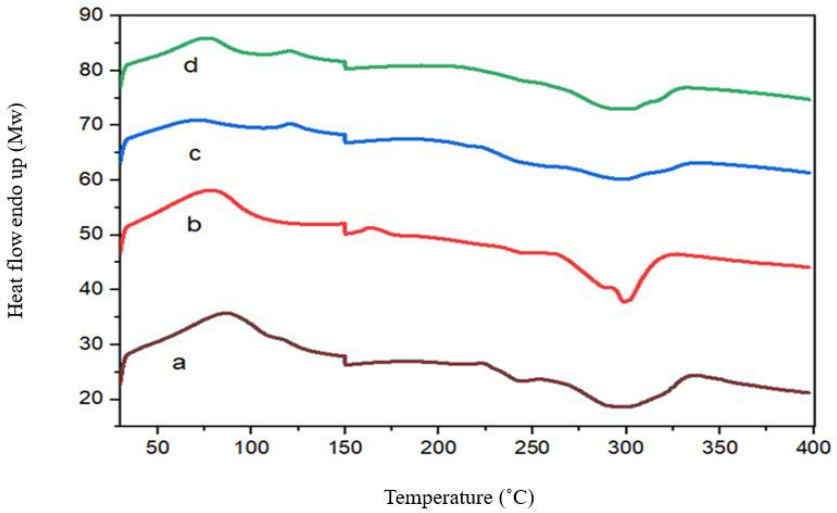

Fig.6. illustrate melting temperature peaks for (a) 60H-40CMC, (b) 60H-40CMC-MMT, (c) 60H-40CMC-3MMT, (d) 60H-40CMC-5MMT.

A small endothermic peak for all nanocomposite films can be seen at 100ºC. This was related to the endothermic peak from temperature 30 ºC to 200 ºC range from the moisture removal when the samples were heated and exhibits the hydrophilic properties of the relevant polymer due to water loss [25]. Compared to the melting temperature T_m of native hemicelluloses, which was between 200ºC and 250ºC [25], the T_m data obtained for nanocomposites films was in the range from 250ºC until 300ºC due to hemicelluloses film modification. An extra endothermic event close to a glass transition was visible at 55–65 ℃ (T_g) in the DSC curve of the films. The curves for the film sample indicated a slight discontinuity in this temperature range. The discontinuity may be related to the sample's glass transition [26].

It is crucial to measure the glass transition (T_g) and the thermal degradation characteristics of the polymers, as they can reflect the performance of the films. The higher molecular weight or cross-linking corresponds to any given polymer's higher strength and glass transition temperature [27]. Based on Table 5, T_g increased as the MMT loading increased. This phenomenon is due to plasticization at a high content loading, disrupting the polymer chain package. The increase in the MMT loading content resulted either in the plasticization effect or the filling of the free volume of the polymer. Thus, it caused a dense polymer package and increased the T_g value [28].

From Figure 6, the peak of nanocomposite films at melting point had slightly shifted to the right as the concentration of MMT increased. This is because the changes in melting and crystallization behavior with the addition of MMT loading result from MMT platelets behaving as nucleating centers and favoring crystallization by providing a higher nucleation density [24]. The melting temperature (T_m) of the nanocomposite films is presented in Table 5. Adding MMT into the hemicelluloses film raised the melting temperature (T_m) of the nanocomposite film. This is due to their crystallinity percentage, as described in the XRD results, which explained that high crystallinity needs more energy to vibrate and break the polymer chain than a low crystallinity material. Based on Figure 6, no significant difference in peak shape was

https://doi.org/10.24191/sl.v18i2.25392

observed between nanocomposite films with the incorporation of MMT loading. However, 3% and 5% MMT loading of nanocomposite films show a broad peak compared to samples without MMT and 1% of MMT loading. This was supported by the value enthalpy of melting in Table 3, which shows the high energy needed as MMT concentration increased. Balakrishnan et al. [29] reported that the incorporation of MMT does not change the melting temperature of the nanocomposite films. As identical peak shapes were observed, this behavior indicates poor dispersion and nucleating activity in the composite system. Comparable results have also been reported for LDPE/RH composite films [24].

Table 4. Melting temperatures of the hemicellulose films.

Samples	T_g (℃)	T_m (℃)	ΔH
60H-40CMC	147.90	266.71	-180.19 J/G
60H-40CMC-MMT	149.39	262.37	-179.44 J/G
60H-40CMC-3MMT	154.82	286.44	-215.43 J/G
60H-40CMC-5MMT	152.62	274.83	-193.46 J/G

Concerning crystallinity, adding up to 5% MMT resulted in a decrease with increasing the MMT loading. A declining trend in crystallinity was observed, which can be attributed to the agglomeration of MMT. This led to the intercalated nanocomposite structure, as if MMT were dispersed homogeneously, and the crystallinity would increase. This was supported by data from the tensile strength, which decreased as the MMT loading increased by 5%. Adding MMT loading can enhance the mechanical and thermal properties of hemicellulose nanocomposite films.

Thermogravimetric analysis (TGA)

TGA analysis measures the material's thermal stability by evaluating the mass loss with rising temperature. Figures 7 and 8 display the nanocomposite films' TGA analysis and DTG profile, respectively. Thermal stability can be articulated within the context of the initial temperature of the decomposition [3], the temperature at the beginning of the decomposition, and the residual substance, as shown in Table 4, along with the outcome of the decomposition in Figure 8. Based on Figures 7 and 8, the blend film (60H-40CMC) and nanocomposite films with the incorporation of 1%,3%, and 5% of MMT loading showed a one-step degradation process represented by a single peak for both the TGA and DTG curves. The samples of the blend and nanocomposites exhibit an initial weight loss of around 100 ℃. In contrast with the blend film, Figure 7 indicates an increase in the thermal stability of the nanocomposite films. It can be noted that at T_{60}, the degradation temperature was higher than the blend films. This showed that incorporating MMT into the blend films can enhance thermal stability. A comparable result was recorded by Chen et al. [7]. A uniform dispersion of the nanofiller in the matrix may be due to the improvement in the thermal properties of the nanocomposite films.

The percentage of residual weight increased as the MMT loading increased. T_{max} of the hemicellulose film composite improved due to the addition of MMT. The range was from 280.67 to 296.33 ℃. However, the thermal stability began to decline with the increase of MMT loading up to 3%. This condition is due to the delamination and exfoliated MMT layers considered to enhance the thermal degradation resistance. Low improvement in thermal degradation with a higher concentration of MMT is because of the agglomeration of MMT as confirmed by XRD observations [24]. The amount of char for residual weight shows the lowest percentage for blend film, with 29.75%. As shown in Table 4, the amount of char increases with the increase of MMT loading. This is attributed to the presence of Silica in MMT,

https://doi.org/10.24191/sl.v18i2.25392

which has a melting point above 3500 °C [24]. It does not decompose under TGA temperature and produces a residue. Based on the observations, delamination or exfoliation of MMT plays a vital role in determining the thermal properties of nanocomposite film. Furthermore, the increment of 3% MMT loading into hemicellulose blend film is an optimum level that, beyond the percent of MMT loading, will cause thermal stability degradation.

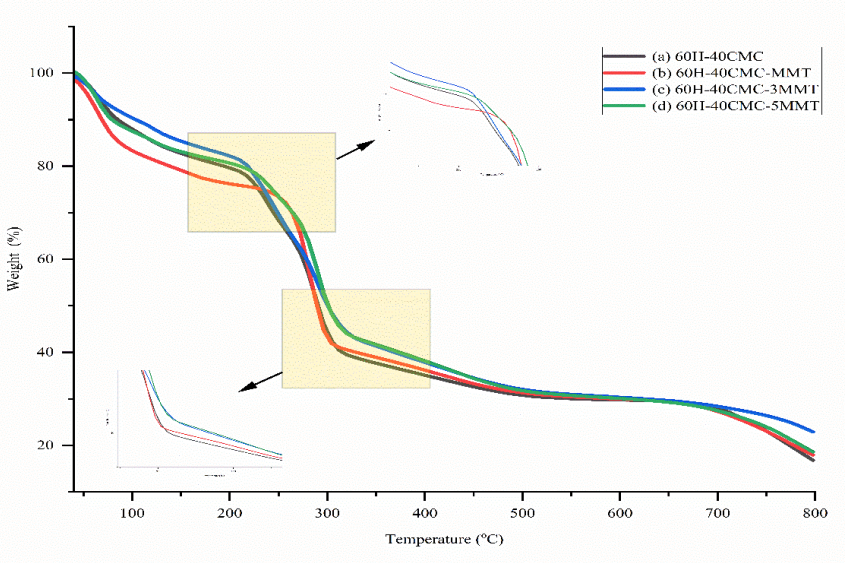

Fig. 7 TGA graph of the blend and nanocomposite films: (a) 60H-40CMC, (b) 60H-40CMC-MMT, (c) 60H-40CMC-3MMT, and (d) 60H-40CMC-5MMT.

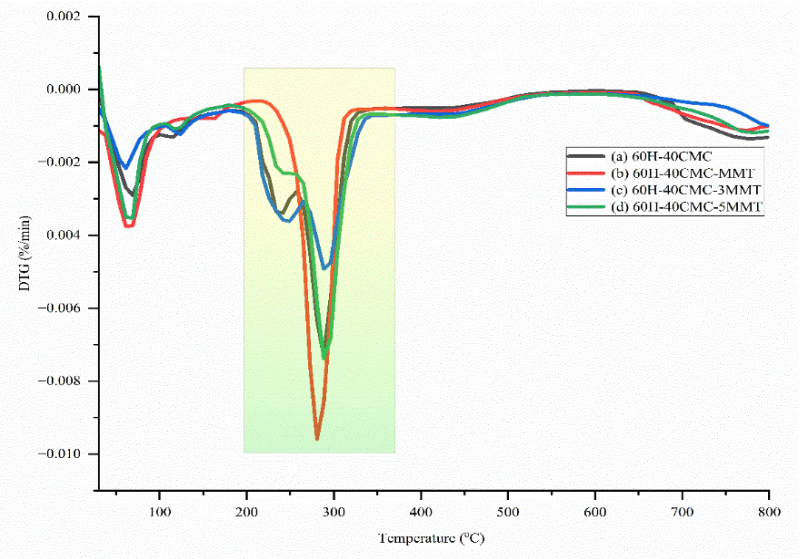

Fig. 8. DTG graph of the blend and nanocomposite films: (a) 60H-40CMC, (b) 60H-40CMC-MMT, (c) 60H-40CMC-3MMT, and (d) 60H-40CMC-5MMT.

https://doi.org/10.24191/sl.v18i2.25392

Table 5 Thermal properties of the blend and nanocomposite films.

Samples	Degadation temperature (℃)			Residual weight (%) at 600 ℃
	T_{10}	T_{60}	T_{max}	
60H-40CMC	84.83	312.00	290.00	29.75
60H-40CMC-MMT	69.16	319.83	280.67	29.96
60H-40CMC-3MMT	100.50	359.00	296.33	30.33
60H-40CMC-5MMT	77.00	366.83	290.32	31.08

CONCLUSION

The incorporation of MMT into hemicellulose-CMC film improved the mechanical properties. The highest tensile strength obtained was at 3% of MMT loading. As MMT loading increased, film surface morphology became dense and rough. FTIR spectroscopy revealed that the intensity peak of the siloxanes group that represented the MMT increased with the addition of MMT loading in the nanocomposite film. In contrast, thermal analysis showed good thermal properties were achieved as MMT loading increased to 3% of MMT concentration. Besides, 3% MMT in the nanocomposite formulation enhanced the hemicellulose-based nanocomposite films' functional and mechanical strength properties, thereby minimizing the water uptake. In general, a hemicellulose-based film with the incorporation of 3% MMT (60H-40CMC-3MMT) was the optimum result, among others. The results projected that the film from empty fruit bunches from oil palm plantations has excellent potential to be used in the production of the renewable packaging industry.

ACKNOWLEDGEMENTS

The authors are grateful to the Bioresource Technology Division of the School of Industrial Technology for the facilities provided during the fabrication of the nanocomposite films. This work was supported by Research University Grant Scheme (RU) 1001/PTEKIND/8011108 allocated by Universiti Sains Malaysia and Fundamental Research Grant Scheme FRGS/1/2019/STG07/USM/02/15 from the Ministry of Higher Education, Malaysia.

AUTHOR'S CONTRIBUTION

Hanis carried out the research and wrote and revised the article. Zaim and Haafiz conceptualized the central research and provided the theoretical framework. Nasrullah, Fazita, and Adilah designed the research and supervised the research progress; Falah and Haafiz anchored the review and revisions and approved the article submission.

CONFLICT OF INTEREST STATEMENT

The authors agree that this research was conducted without any self-benefits or commercial or financial conflicts and declare the absence of conflicting interests with the funders.

REFERENCES

1. Faruk, O., Bledzki, A. K., Fink, H. P., & Sain, M. (2014). Progress report on natural fiber reinforced composites. *Macromolecular Materials and Engineering*, 299, 9-26. https://doi.org/10.1002/mame.201300008

https://doi.org/10.24191/sl.v18i2.25392

2. Dicker, M. P. M., Duckworth, P. F., Baker, A. B., Francois, G., Hazzard, M. K., & Weaver, P. M. (2014). Green composites: A review of material attributes and complementary applications. *Composites Part A: Applied Science and Manufacturing*, 56, 280-289. https://doi.org/10.1016/j.compositesa.2013.10.014
3. Zailuddin, N. L. I., Osman, A. F., Husseinsyah, S., Ariffin, Z., & Badrun, F. H. (2018). Mechanical properties and X-ray diffraction of oil palm empty fruit bunch all-nanocellulose composite films. *Proceedings of the Second International Conference on the Future of ASEAN (ICoFA) 2017, 2*, 505-514. https://doi.org/10.1007/978-981-10-8471-3_50
4. Rosli, N. S., Harun, S., Jahim, J. M., & Othaman, R. (2017). Pencirian kimia dan fizikal bagi tandan kosong buah kelapa sawit. *Malaysian Journal of Analytical Sciences*, 21(1) 188-196. https://doi.org/10.17576/mjas-2017-2101-22
5. Faizi, M. K., Shahriman, A. B., Majid, M. S. A., Shamsul, B. M. T., Nawawi, A. S. M., Zunaidi, I., Wan, W. K. (2018). The effect of multiple surface treatments on oil palm empty fruit bunch (OPEFB) fibre structure. *IOP Conference Series: Materials Science and Engineering*, 429, 012005. https://doi.org/10.1088/1757-899X/429/1/012005
6. Haafiz, K. M., Taiwo, O. F. A., Razak, N., Rokiah, H., Hazwan, H. M., Rawi, N. F. M., & Khalil, H. P. S. A. (2019). Development of green MMT-modified hemicelluloses based nanocomposite film with enhanced. *Bioresources*, 14(4), 8029-8047. DOI:10.15376/biores.14.4.8029-8047
7. Chen, G.G., Qi, X.M., Guan, Y., Peng, F., Tao, C.L., and Sun, R.C. (2016). High strength hemicelluloses-based nanocomposites film for food packaging applications. *ACS Sustainable Chemistry and Engineering* 4(4), 1985-1993. DOI:10.1021/acssuschemeng.5b01252
8. Bao, Y., Zhang, H., Luan, Q., Zheng, M., Tang, H., & Huang, F. (2018). Fabrication of cellulose nanowhiskers reinforced chitosan-xylan nanocomposite films with antibacterial and antioxidant activities. *Carbohydrate Polymers*, 184, 66–73. https://doi.org/10.1016/J.CARBPOL.2017.12.051
9. Zhao, Y., Sun, H., Yang, B., & Weng, Y. (2020). Hemicellulose-based film: Potential green films for food packaging. *Polymers*, 12(8), 1775. https://doi.org/10.3390/polym12081775
10. Chen, G.G., Qi, X.M., Li, M.P., Guan, Y., Bian, J., Peng, F., and Sun, R.C. (2015). Hemicelluloses/montmorillonite hybrid films with improved mechanical and barrier properties. *Scientific Reports*, 5, 16405. https://doi.org/10.1038/srep16405
11. Qi, X.M., Liu, S.Y., Chu, F.B., Pang, S., Liang, Y.R., Guan, Y., Sun, R.C. (2015). Preparation and characterization of blended films from quaternized hemicelluloses and carboxymethyl cellulose. *Materials (Basel, Switzerland)*, *9*, 4. https://doi.org/10.3390/ma9010004
12. Gao, H., Rao, J., Guan, Y., Li, W., Zhang, M., Shu, T., & Lv, Z. (2018). Investigation of the thermo-mechanical properties of blend films based on hemicelluloses and cellulose. *International Journal of Polymer Science*, 2018, 1–10. https://doi.org/10.1155/2018/9620346
13. Wang, B., Yang, X., Qiao, C., Li, Y., Li, T., & Xu, C. (2018). Effects of chitosan quaternary ammonium salt on the physicochemical properties of sodium carboxymethyl cellulose-based films. *Carbohydrate Polymers*, 184, 37–46. https://doi.org/10.1016/J.CARBPOL.2017.12.030
14. Majeed, K., Hassan, A., Bakar, A. A., & Jawaid, M. (2016). Effect of montmorillonite (MMT) content on the mechanical, oxygen barrier, and thermal properties of rice husk/MMT hybrid filler-filled low-density polyethylene nanocomposite blown films. *Journal of Thermoplastic Composite Materials*, *29*(7), 1003–1019. https://doi.org/10.1177/0892705714554492
15. Makwana, D., Castano, J., Somani, R.S., and Bajaj, H.C. (2018). Characterization of Agar-CMC/Ag-MMT nanocomposite and evaluation of antibacterial and mechanical properties for packaging applications. *Arabian Journal of Chemistry*, *13* (1), 3092-3099. https://doi.org/10.1016/j.arabjc.2018.08.017
16. Binti, N. H., & Halim, A. (2010). Characterization of physico-chemical and film properties of hemicelluloses from oil palm frond (*Elaeis Guineensis*). MSc Thesis., Malaysian Science University.

https://doi.org/10.24191/sl.v18i2.25392

17. Majeed, K., Hassan, A., Bakar, A. A., & Jawaid, M. (2016). Effect of montmorillonite (MMT) content on the mechanical, oxygen barrier, and thermal properties of rice husk/MMT hybrid filler-filled low-density polyethylene nanocomposite blown films. *Journal of Thermoplastic Composite Materials*, *29*(7), 1003–1019. https://doi.org/10.1177/0892705714554492
18. Dwivedi, C., Pandey, I., Pandey, H., Ramteke, P. W., Pandey, A. C., Mishra, S. B., & Patil, S. (2017). Electrospun nanofibrous scaffold as a potential carrier of antimicrobial therapeutics for diabetic wound healing and tissue regeneration. *Nano- and Microscale Drug Delivery Systems*, 9, 147–164. https://doi.org/10.1016/B978-0-323-52727-9.00009-1
19. Kasirga, Y., Oral, A., & Caner, C. (2012). Preparation and characterization of chitosan/montmorillonite-K10 nanocomposites films for food packaging applications. *Polymer Composites*, 33(11), 1874–1882. https://doi.org/10.1002/pc.22310
20. Saputra, A. H., Qadhayna, L., & Pitaloka, A. B. (2014). Synthesis and characterization of carboxymethyl cellulose (CMC) from water hyacinth using ethanol-isobutyl alcohol mixture as the solvents. *International Journal of Chemical Engineering and Applications*, *5*(1), 36–40. https://doi.org/10.7763/IJCEA.2014.V5.347
21. Maina, E., Wanyika, H., Gachanja, A., & Marikah, D. (2016). Instrumental characterization of montmorillonite clays by x-ray fluorescence spectroscopy, Fourier transform infrared spectroscopy, x-ray diffraction and UV/visible spectrophotometry. *Journal of Agriculture, Science and Technology*, 17.
22. Madejová, J., & Komadel, P. (2001). Baseline studies of the clay minerals society source clays: Infrared methods. *Clays and Clay Minerals*, 49, 410-432, https://doi.org/10.1346/CCMN.2001.0490508
23. Tajeddin. (2016). Preparation and characterization (Mechanical and water absorption properties) of CMC/PVA/Clay nanocomposite films. *J. Chem. Chem. Eng*, 35,3.Retrieved from http://www.ijcce.ac.ir/article_22053_3ee66f57d4f254318f9440b37743a850.pdf
24. Rosnan, R. M., & Arsad, A. (2013). Effect of MMT concentrations as reinforcement on the properties of recycled PET/HDPE nanocomposites. *Journal of Polymer Engineering*, 33(7), 1-9. https://doi.org/10.1515/polyeng-2013-0107
25. Quilaqueo Gutiérrez, M., Echeverría, I., Ihl, M., Bifani, V., & Mauri, A. N. (2012). Carboxymethylcellulose–montmorillonite nanocomposite films activated with murta (Ugni molinae Turcz) leaves extract. *Carbohydrate Polymers*, 87(2), 1495–1502. https://doi.org/10.1016/j.carbpol.2011.09.040
26. Hartman, J., Albertsson, A.-C., Lindblad, M. S., & Sjöberg, J. (2006). Oxygen barrier materials from renewable sources: Material properties of softwood hemicellulose-based films. *Journal of Applied Polymer Science*, 100(4), 2985–2991. https://doi.org/10.1002/app.22958
27. Palamae, S., Dechatiwongse, P., Choorit, W., Chisti, Y., & Prasertsan, P. (2017). Cellulose and hemicellulose recovery from oil palm empty fruit bunch (EFB) fibers and production of sugars from the fibers. *Carbohydrate Polymers*, 155, 491-497. https://doi.org/10.1016/j.carbpol.2016.09.004
28. Corcione, C., & Frigione, M. (2012). Characterization of nanocomposites by thermal analysis. *Materials*, 5(12), 2960–2980. https://doi.org/10.3390/ma5122960
29. Balakrishnan, H., Hassan, A., Imran, M., & Wahit, M. U. (2012). Toughening of polylactic acid nanocomposites: A short review. *Polymer-Plastics Technology* Polylactic Acid Nanocomposites: A Short Review. *Polymer-Plastics Technology and Engineering*, 51(2), 175–192. https://doi.org/10.1080/03602559.2011.618329

https://doi.org/10.24191/sl.v18i2.25392